Combined synchrotron X-ray radiography and tomography study of water transport in gas diffusion layers

Henning Markötter[a,*], Ingo Manke[a], Jan Haußmann[b], Tobias Arlt[a], Merle Klages[b], Philipp Krüger[b,1], Christoph Hartnig[b,2], Joachim Scholta[b], Bernd R. Müller[c], Heinrich Riesemeier[c], John Banhart[a,d]

[a] Helmholtz-Zentrum Berlin (HZB), Hahn-Meitner-Platz 1, 14109 Berlin, Germany
[b] Zentrum für Sonnenenergie- und Wasserstoff-Forschung Baden-Württemberg (ZSW), Helmholtzstraße 8, 89081 Ulm, Germany
[c] Bundesanstalt für Materialforschung und –prüfung (BAM), Unter den Eichen 87, 12205 Berlin, Germany
[d] Technische Universität Berlin (TU-Berlin), Straße des 17. Juni 135, 10623 Berlin, Germany
[1] present address: Consulectra Unternehmensberatung GmbH, Hamburg, Germany
[2] present address: Chemetall GmbH, Frankfurt, Germany

*Corresponding author:
Henning Markötter
Helmholtz-Zentrum Berlin (HZB), Hahn-Meitner-Platz 1, 14109 Berlin, Germany
Tel.: +49 30 8062 42826
e-mail: henning.markoetter@helmholtz-berlin.de

Abstract
Synchrotron X-ray radiography and tomography investigations of a custom-made polymer electrolyte membrane fuel cell optimised for visualisation purposes are presented. The 3D water distribution and transport pathways in the porous carbon fibre gas diffusion layers (GDLs) were investigated. We found that water is not only moving from the GDL into the channel, but can also take the opposite way, i.e. from the channel into free pore space of the GDL. Such movement of water into the opposite direction has been subject of speculations but has so far not yet been reported and might bring new insights into the general water transport behaviour, which might give new aspects to the general description of water transport processes and influence modelling assumptions to describe the process taking place in the GDL.

1. Introduction

Fuel cells enable the operation of vehicles without CO_2 emissions with an electric efficiency of more than 60 %. The most promising fuel cell type for the automotive sector is the low temperature polymer electrolyte membrane fuel cell (PEMFC). In PEMFCs, hydrogen and oxygen react to water and convert chemical energy into thermal and electrical energy [1-4]. On the anode side hydrogen is oxidized and protons are formed, which recombine with oxygen at the cathodic catalyst, where water is produced. In low-temperature PEMFCs water management plays an important role: On the one hand, only sufficiently humidified membranes are proton conductive. On the other hand, flooding of the flow field channels and the gas diffusion layers (GDLs) are significant sources of power loss and strongly affect materials aging [5]. Thus, a thorough insight into the fundamental mechanisms of liquid water evolution and transport is needed for component development. In the past years, interest in such issues has grown continuously [6-11]. Until now, only few techniques suitable for in-situ investigation are available. Neutron and synchrotron X-ray imaging turned out to be very useful to study water distribution and media transport in fuel cells [12-17]. When high spatial and temporal resolutions are required, (synchrotron) X-rays have to be used [18-31]. Images with pixels as small as 1 μm give a clear insight into small features such as pores. Compared to neutrons the flux of the synchrotron beam allows faster fuel cell measurements with shorter exposure times down to about 0.1 s per radiograph.

2.   Synchrotron X-ray tomography

Radiography and tomography were combined in order to investigate both water transport dynamics (two-dimensionally) and the stationary 3D water distribution in the cell [32]. This approach allows to link dynamic processes to the features of the related material in 3D.

2.1.   Fuel cell

A specific requirement of the employed tomographic imaging setup is that the cell section under investigation has to fit fully into the field of view of about 14 mm. To meet this requirement an adapted fuel cell was designed and manufactured. The cell materials have been chosen to account for an attenuation to allow for sufficient beam transmission. Therefore the metallic endplates were replaced by acrylic glass in the area to be visualized as described elsewhere [33], where first measurements with this cell have been presented. On the cathode and anode side, a single serpentine flow field channel, (channel cross section: 500 µm × 500 µm) has been machined into graphite composite plates. SGL GROUP 10BC GDLs containing 5 wt.% Teflon (PTFE) equipped with a micro porous layer (MPL) were placed on both sides of a catalyst-coated Nafion 112 proton conducting membrane. The catalyst load of 0.51 mg cm^{-2} on the anode and 0.57 mg cm^{-2} on the cathode consisted of a mixture of 60 % carbon and 40 % platinum. Cell design and first results are described in [32, 33]. Cell operation was arranged with utilization ratios of 40 % for the cathode and 50 % for the anode side at 50 °C cell temperature. During radiography, the cell was operated at current densities ranging from 40 to 160 mA cm^{-2}. Prior to the tomographic imaging, cell operation was stopped and the inlets and outlets were closed to conserve the present water distribution.

2.2.   Experimental setup

Measurements were carried out at the BAMline at Bessy II (electron storage ring in Berlin, Germany) [34]. The experimental station delivers an X-ray beam in a wide energy range with a horizontal beam width of up to 20 mm. A dual multilayer monochromator with an energy resolution of about $\Delta E/E = 10^{-2}$ was used to obtain a monochromatic 15 keV X-ray beam. A 4008 × 2672 pixel PCO4000 camera was used to capture images of 19.2 × 12.8 mm² in size. A physical resolution of 10 µm is obtained, which is sufficiently high to resolve even small water clusters inside the pores of the GDL. Exposure times of 1 s for each of the 1800 projections were chosen. Two projections of the cell are shown in Fig. 1.

3.   Results

Fig. 2a-d show a radiographic sequence of a selected cell detail, more precisely a turn of the cathodic flow field channel. First, a water droplet sticks to the channel wall (Fig. 2a,b; red arrow). At 81 s in the sequence, this droplet has disappeared, most likely flushed away by another water droplet that was moving at high velocity through the channel. At the same time, a water accumulation appears beneath the land (Fig. 2c,d; black arrow), indicating the existence of a larger pore space in the GDL.

The dynamics of local water accumulation at these two locations, marked by a black and a red circle in Fig. 2a, were studied in further detail (Fig. 2e). The water droplet in the channel shows an almost periodic behaviour (Fig. 2e; red graph). It slowly grows up about 100 µm in depth until it suddenly disappears in accordance to Fig. 2b,c after which a new cycle begins. On the other hand, the black line in Fig. 2e shows only little variation except at one instant, namely at about 81 s, when the water layer thickness suddenly increases. This implies that the pore space has been filled (Fig. 2c) at the same time at which the channel droplet disappears. It is expected that the water droplet has been flushed away by a passing water drop, while at the same time some water has been transferred into the open pore space beneath the land.

Starting from this two-dimensional study of the inverse water transport the sample area has been investigated in more detail in the tomographic 3D dataset of the cell. The sample area given in Fig. 2 was identified in the corresponding tomogram. In Fig. 3 one can clearly see a large pore space beneath the land close to the flow field channel (encircled in Fig. 3b,d). The pore provides a large opening into the channel with a diameter of about 100 μm. This large opening results in a reduced transport resistance for liquid water allowing the transfer from the channel into the GDL and vice versa. The pore is roughly $100 \times 200 \times 250$ μm³ large (x, y, z). A quantification of the water amount in Fig. 2e reveals that the water layer thickness in x direction changes by about 40 to 50 μm, which implies that the pore had been only partially filled by the flushing event shown in Fig. 2c.

The water distribution in the respective GDL pore was further studied at four different current densities shown in Fig. 3e-h, namely 40, 80, 120 and 160 mA cm^{-2}. Some small water droplets can be found at lower current densities. At 160 mA cm^{-2}, the pore was completely filled with water, see Fig. 3h.

4. Discussion

Large pores which are connected to the channel of the flow field might serve as a reservoir or collecting vessel containing product water that was transported from the catalyst layer through the GDL towards the flow field channel, which is in the next step expelled to the channel. Once the situation occurs that this (most probably hydrophilic spot) is empty while a larger droplet passes the channel the reservoir can be filled inversely (Fig. 2f) suggesting that water can also move from the channel into larger GDL pores. The necessary pressure for water to pass an opening built by fibres is calculated by Zhou [35] via an approach using a fibre fence structure. For pores with an opening of 100 μm in diameter to the channel only a pressure of less than 2 kPa is needed to bring water from the channel into the pore space and in turn explains why a filling of smaller pores has not been observed. The conditions in the channel turnings are favourable for the build-up of water droplets: On the one hand, turbulences which might occur at these positions favour the formation of liquid water. From these images and the water transport behaviour, the previously considered uni-directional water transport can be seen from another point of view describing a bi-directional transport: If a sufficient wide (and most likely sufficiently hydrophilic) pore space is accessible which in turn requires a sufficiently low pressure for water to enter, water can also be transported from the flow field channel to the gas diffusion media. Unfortunately, from the images taken so far, the fate of the water volume which has been transported back to the pore has not been identified but it's most likely that in the next step a droplet will be formed emptying this pore. The situation is probable once the water pressure inside the GDL is sufficiently high.

5. Summary and Conclusions

A study of water transport processes in PEMFCs by means of synchrotron X-ray imaging was presented. The combination of dynamic radiographies with static 3D tomographies gives access to a three-dimensional reconstruction of the dynamic processes observed. In the presence of larger water amounts in the flow field channels, water could not only move from the GDL into the channel but was also transported inversely back into the GDL pore space. These findings are expected to contribute to simulation studies and to the choice of GDL materials in the future.

References:
[1] Vielstich W, Lamm A, Gasteiger HA. Handbook of Fuel Cells – Fundamentals, Technology and Applications. Chichester: John Wiley & Sons; 2003.
[2] Steele BCH, Heinzel A. Materials for fuel-cell technologies. Nature. 2001;414:345-52.
[3] Carrette L, Friedrich KA, Stimming U. Fuel Cells - Fundamentals and Applications. Fuel Cells. 2001;1:5-39.
[4] Wang C-Y. Fundamental Models for Fuel Cell Engineering. Chem Rev. 2004;104:4727-66.
[5] Ohyagi S, Matsuda T, Iseki Y, Sasaki T, Kaito C. Effects of operating conditions on durability of polymer electrolyte membrane fuel cell Pt cathode catalyst layer. J Power Sources. 2011;196:3743-9.
[6] Pasaogullari U, Wang C-Y. Two-Phase Modeling and Flooding Prediction of Polymer Electrolyte Fuel Cells. J Electrochem Soc. 2005;152:A380-A90.
[7] Kulikovsky AA, Wüster T, Egmen A, Stolten D. Analytical and Numerical Analysis of PEM Fuel Cell Performance Curves. J Electrochem Soc. 2005;152:A1290.
[8] Lin G, He W, Nguyen TV. Modeling Liquid Water Effects in the Gas Diffusion and Catalyst Layers of the Cathode of a PEM Fuel Cell. J Electrochem Soc. 2004;151:A1999-A2006.
[9] Ziegler C, Yu HM, Schumacher JO. Two-Phase Dynamic Modeling of PEMFCs and Simulation of Cyclo-Voltammograms. J Electrochem Soc. 2005;152:A1555-A67.
[10] Berg P, Promislow K, Pierre JS, Stumper J, Wetton B. Water Management in PEM Fuel Cells. J Electrochem Soc. 2004;151:A341-A53.
[11] Litster S, Sinton D, Djilali N. Ex situ visualization of liquid water transport in PEM fuel cell gas diffusion layers. J Power Sources. 2006;154:95-105.
[12] Banhart J. Advanced Tomographic Methods in Materials Research and Engineering. Oxford, UK: Oxford University Press; 2008.
[13] Banhart J, Borbely A, Dzieciol K, Garcia-Moreno F, Manke I, Kardjilov N, et al. X-ray and neutron imaging - Complementary techniques for materials science and engineering. International Journal of Materials Research. 2010;101:1069-79.
[14] Manke I, Markötter H, Tötzke C, Kardjilov N, Grothaussmann R, Dawson M, et al. Investigation of energy-relevant materials with synchrotron X-rays and neutrons. Adv Eng Mater. 2011;13:712-29.
[15] Kardjilov N, Manke I, Hilger A, Strobl M, Banhart J. Neutron imaging in materials science. Materials Today. 2011;14:248-56.
[16] Schröder A, Wippermann K, Lehnert W, Stolten D, Sanders T, Baumhöfer T, et al. The influence of gas diffusion layer wettability on direct methanol fuel cell performance: A combined local current distribution and high resolution neutron radiography study. J Power Sources. 2010;195:4765-71.
[17] Kardjilov N, Hilger A, Manke I, Strobl M, Dawson M, Banhart J. New trends in neutron imaging. Nuclear Instruments and Methods in Physics Research Section A: Accelerators, Spectrometers, Detectors and Associated Equipment. 2009;605:13-5.
[18] Manke I, Hartnig C, Grünerbel M, Lehnert W, Kardjilov N, Haibel A, et al. Investigation of water evolution and transport in fuel cells with high resolution synchrotron x-ray radiography. Appl Phys Lett. 2007;90:174105.
[19] Hartnig C, Manke I, Schloesser J, Krüger P, Kuhn R, Riesemeier H, et al. High resolution synchrotron X-ray investigation of carbon dioxide evolution in operating direct methanol fuel cells. Electrochem Commun. 2009;11:1559-62.
[20] Manke I, Hartnig C, Kardjilov N, Riesemeier H, Goebbels J, Kuhn R, et al. In situ Synchrotron X-ray Radiography Investigations of Water Transport in PEM Fuel Cells. Fuel Cells. 2010;10:26-34.

[21] Sinha PK, Mukherjee PP, Wang CY. Impact of GDL structure and wettability on water management in polymer electrolyte fuel cells. Journal of Materials Chemistry. 2007;17:3089-103.

[22] Sinha PK, Halleck P, Wang C-Y. Quantification of Liquid Water Saturation in a PEM Fuel Cell Diffusion Medium Using X-ray Microtomography. Electrochemical and Solid-State Letters. 2006;9:A344-A8.

[23] Thiedmann R, Hartnig C, Manke I, Schmidt V, Lehnert W. Local Structural Characteristics of Pore Space in GDLs of PEM Fuel Cells Based on Geometric 3D Graphs. J Electrochem Soc. 2009;156:1339-47.

[24] Sasabe T, Tsushima S, Hirai S. In-situ visualization of liquid water in an operating PEMFC by soft X-ray radiography. International Journal of Hydrogen Energy. 2010;35:11119-28.

[25] Sasabe T, Deevanhxay P, Tsushima S, Hirai S. Soft X-ray visualization of the liquid water transport within the cracks of micro porous layer in PEMFC. Electrochem Commun. 2011;13:638-41.

[26] Becker Jr, Flückiger R, Reum M, Büchi FN, Marone F, Stampanoni M. Determination of Material Properties of Gas Diffusion Layers: Experiments and Simulations Using Phase Contrast Tomographic Microscopy. J Electrochem Soc. 2009;156:B1175.

[27] Kuhn R, Scholta J, Krüger P, Hartnig C, Lehnert W, Arlt T, et al. Measuring device for synchrotron X-ray imaging and first results of high temperature polymer electrolyte membrane fuel cells. J Power Sources. 2011;196:5231-9.

[28] Maier W, Arlt T, Wannek C, Manke I, Riesemeier H, Krüger P, et al. In-situ synchrotron X-ray radiography on high temperature polymer electrolyte fuel cells. Electrochem Commun. 2010;12:1436-8.

[29] Guan Y, Li WJ, Gong YH, Liu G, Gelb J, Zhang XB, et al. The study of the reconstructed three-dimensional structure of a solid-oxide fuel-cell cathode by X-ray nanotomography. Journal of Synchrotron Radiation. 2010;17:782-5.

[30] Je J, Kim J, Kaviany M, Son SY, Kim M. X-ray tomography of morphological changes after freeze/thaw in gas diffusion layers. Journal of Synchrotron Radiation. 2011;18:743-6.

[31] Ostadi H, Rama P, Liu Y, Chen R, Zhang XX, Jiang K. Influence of threshold variation on determining the properties of a polymer electrolyte fuel cell gas diffusion layer in X-ray nano-tomography. Chemical Engineering Science. 2010;65:2213-7.

[32] Markötter H, Manke I, Krüger P, Arlt T, Haussmann J, Klages M, et al. Investigation of 3D water transport paths in gas diffusion layers by combined in-situ synchrotron X-ray radiography and tomography. Electrochem Commun. 2011;13:1001-4.

[33] Krüger P, Markötter H, Haussmann J, Klages M, Arlt T, Banhart J, et al. Synchrotron X-ray tomography for investigations of water distribution in polymer electrolyte membrane fuel cells. Journal of PowerSources. 2011;196:5250-5.

[34] Görner W, Hentschel MP, Müller BR, Riesemeier H, Krumrey M, Ulm G, et al. BAMline: the first hard X-ray beamline at BESSY II. Nuclear Instruments and Methods in Physics Research Section A: Accelerators, Spectrometers, Detectors and Associated Equipment. 2001;467-468:703-6.

[35] Zhou P, Wu CW. Liquid water transport mechanism in the gas diffusion layer. J Power Sources. 2010;195:1408-15.
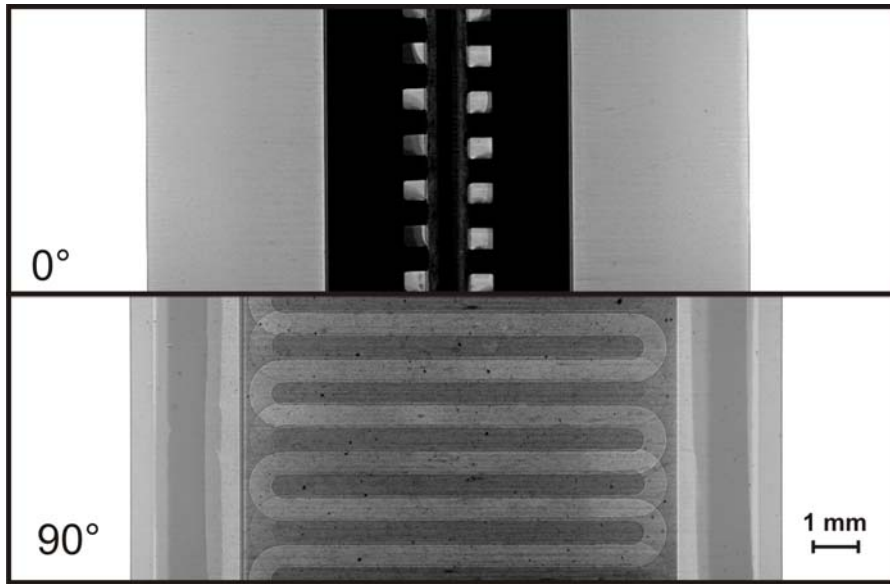
Fig. 1: Selected normalized radiographs used for tomographic reconstruction of the fuel cell adapted to the boundary conditions of synchrotron tomography.
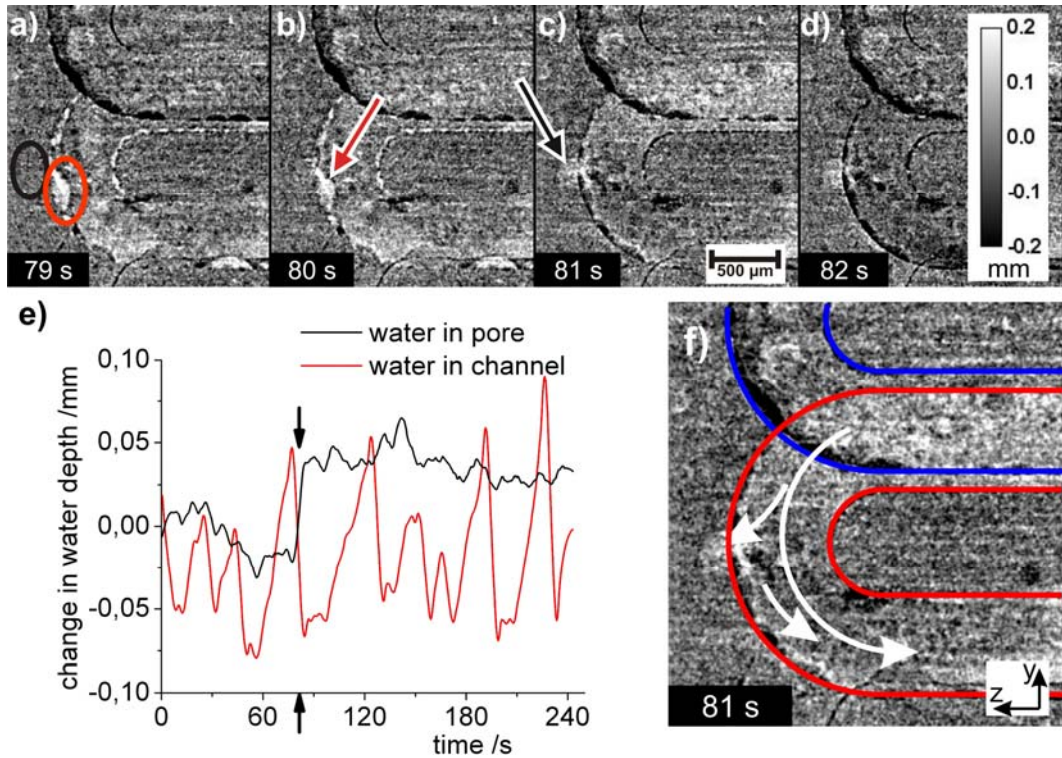
Fig. 2: a-d) Series of radiographs obtained at 160 mA cm⁻², where the water thickness is encoded as gray value. A big pore space next to the cathode channel is filled with water passing the channel. e) Water depth of two positions marked in a) are given. A drop in the channel (red line) builds up and is carried away several times. The position at the big pore next to the channel (black line) is filled in one instance. f) Sketch of this process.
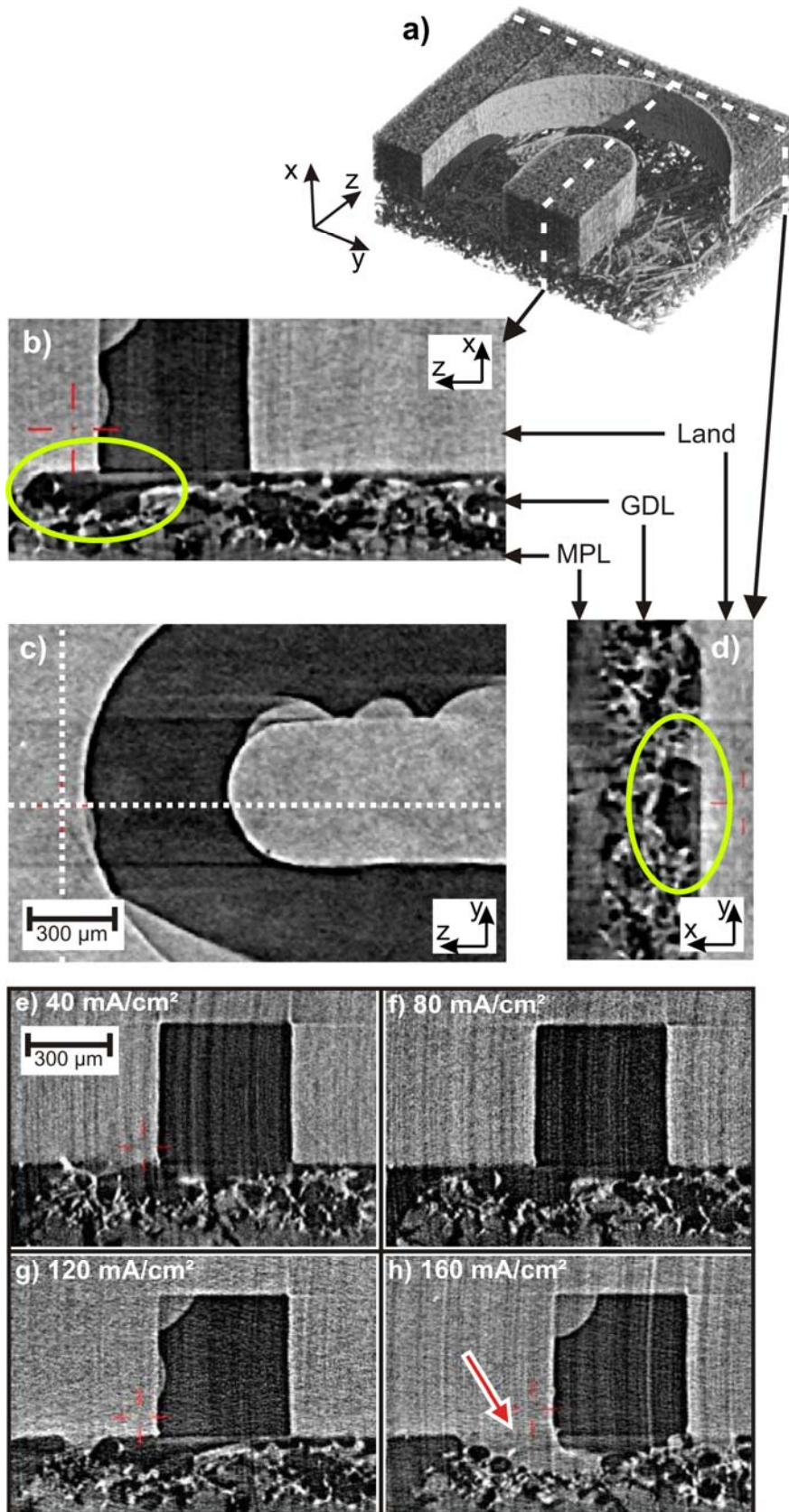
Fig. 3: a) cutout of a tomogram b-d) slices of the tomogram at a relatively big pore space in all three directions. e-h) slices of tomograms at different current densities.